

## Oxygen-vacancy sites on $\text{TiO}_2(100)1 \times 3$ using surface core-level-shift photoelectron diffraction

P. J. Hardman, N. S. Prakash,\* C. A. Muryn, G. N. Raikar,<sup>†</sup> A. G. Thomas, A. F. Prime, and G. Thornton

*Interdisciplinary Research Centre in Surface Science and Department of Chemistry, Manchester University, Manchester M13 9PL, United Kingdom*

R. J. Blake

*Science and Engineering Research Council, Daresbury Laboratory, Warrington WA4 4AD, United Kingdom*

(Received 29 January 1993)

Surface core-level-shift photoelectron diffraction has been used to determine the position of oxygen vacancies on rutile  $\text{TiO}_2(100)1 \times 3$ . Ti  $3p$  photoelectrons associated with Ti atoms adjacent to oxygen vacancies were used as the diffraction source. The angle-scanning mode at fixed photon energy was employed to provide maximum surface sensitivity. By comparison with multiple-scattering calculations, the data indicate that vacancies are located in the topmost layer of a microfacet structure proposed on the basis of grazing-incidence x-ray diffraction data.

While much is known about the structure of oxygen vacancies in metal oxides,<sup>1</sup> little is known about their surface structure.<sup>2</sup> These defects play an important role in determining the physical and chemical surface properties of the materials and hence influence their technological applications.

In a recent scanning tunneling microscopy (STM) study of rutile  $\text{TiO}_2(100)1 \times 3$  (Ref. 3) we identified individual oxygen vacancies, which form an ordered array on this surface. These data are consistent with photoemission results,<sup>4</sup> which evidence the creation of vacancies associated with the  $1 \times 3$  reconstruction. They are also consistent with a microfacet model of the surface deduced from grazing incidence x-ray diffraction (GXR),<sup>5</sup> modified to introduce O vacancies. However, the STM data do not provide a definitive location of these vacancies in relation to the microfacet morphology derived from GXR. In this paper we describe a surface core-level-shift photoelectron diffraction study which locates the position of the vacancies.

The combination of surface core-level-shift spectroscopy (SCLS) and photoelectron diffraction (PED) has been shown to be a powerful tool in the elucidation of clean surface structures.<sup>6,7</sup> This work represents an extension of its use to a new area of application, namely, the location of surface O vacancies on a metal oxide. Our PED data are compared with the results of multiple-scattering calculations for possible structural models. This allows us to place O vacancies at the top of the  $\text{TiO}_2(100)1 \times 3$  microfacets.

PED experiments employed the grazing incidence monochromator ( $30 \leq h\nu \leq 200$  eV) (Ref. 8) on station 6.1 at the Synchrotron Radiation Source, Daresbury Laboratory. A VSW HA100 hemispherical electron energy analyzer with multichannel detection was used in the experimental chamber, the base pressure of which was  $\leq 10^{-10}$  mbar. The angular dependence of the Ti  $3p$  signal was used to monitor diffraction at a fixed photon en-

ergy, 110 eV, with the sample at 295 K. This energy was selected to maximize the surface sensitivity, the photoelectron kinetic energy being close to the escape depth minimum. The combined (monochromator plus analyzer) energy resolution of the measurements was about 0.7 eV [FWHM (full width at half maximum)]. The angular resolution of the analyzer, the entrance axis of which was at  $90^\circ$  to the incoming light in the horizontal plane, was  $\pm 2^\circ$  (FWHM). Normalization to the incident photon flux was accomplished using the drain current from a W mesh placed between the monochromator and sample. Ti  $3p$  photoemission spectra were recorded in  $3^\circ$  intervals of azimuthal emission angle  $\phi$  from  $-66^\circ$  to  $102^\circ$  ( $0^\circ \equiv [010]$ ) at a polar angle of emission,  $\theta = 20^\circ$ , and  $-9^\circ \leq \phi \leq 180^\circ$  at  $\theta = 40^\circ$ .

Sample preparation followed an established method to form a clean  $\text{TiO}_2(100)1 \times 3$  surface,<sup>4</sup> which involves annealing the stoichiometric  $1 \times 1$  surface at  $\sim 1100$  K. The resulting surface had a total contamination level of  $< 1\%$ , as judged by Auger spectroscopy, and exhibited a well-defined  $1 \times 3$  low-energy electron diffraction (LEED) pattern.

The Ti  $3p$  photoemission spectrum of  $\text{TiO}_2(100)1 \times 3$  shown in Fig. 1 contains three features, a "bulk" peak at 66.7-eV kinetic energy, a satellite feature at 65.1 eV, and a SCLS peak arising from O vacancies at 68.5 eV. The assignment of the 65.1-eV feature to an energy-loss process follows a detailed study of surface core-level shifts of  $\text{TiO}_2$  surfaces.<sup>9</sup> The "bulk" feature will also contain a contribution from surface Ti atoms not associated with O vacancies. For the purposes of this work it is sufficient to note that the corresponding spectrum of the stoichiometric  $1 \times 1$  surface differs only in that the SCLS peak at 68.5 eV is absent. This feature can be associated with reduced, nominally  $\text{Ti}^{3+}$  species adjacent to O vacancies. The separation from the bulk peak of 1.8 eV is identical to that observed on reducing a rutile  $\text{TiO}_2(110)$  surface.<sup>10</sup>

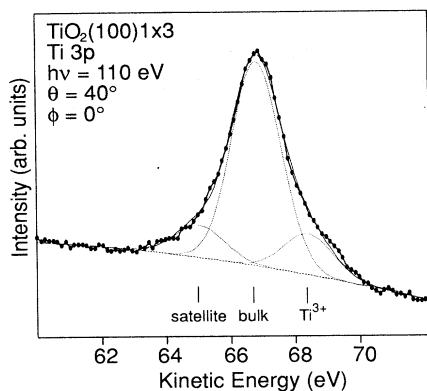


FIG. 1. A typical Ti 3p core-level spectrum of  $\text{TiO}_2(100)1 \times 3$  showing the result of curve-fitting to three Gaussian components and the background.

As we show below, the use of the SCLS peak to monitor diffraction rather than the total Ti 3p peak provides significantly enhanced sensitivity to the O-vacancy site. This is despite the decreased signal-to-noise ratio which is introduced by the need to curve-fit the spectra. Spectra were simultaneously fitted with a background and three symmetric Gaussian components all with a FWHM of 1.72 eV (see Fig. 1). The background shown in Fig. 1 produced the most consistent results, being a linear combination of a sine and a third-order polynomial function. Resulting diffraction curves for the bulk and SCLS features are shown in Fig. 2, where a clear difference between the two is apparent. The variation in intensity of the satellite peak has the same form as the bulk feature. For comparison with theoretical calculations the experimental data were averaged about  $0^\circ$  in azimuthal angle.

In Fig. 2 the experimental data are compared with the results of multiple-scattering calculations for the four structural models illustrated in Fig. 3. The resulting  $R$  factors<sup>11</sup> are shown in Table I. Three of the models are based on the microfacet model proposed from GXR<sup>5</sup>, modified to include O-vacancy sites. Three vacancy sites were considered. The first, which involves the removal of O atoms labeled *A* in Fig. 3(a), places the vacancies in the top layer of the surface. The remaining two sites, labeled *B*, *C* in Fig. 3(a) involve the removal of bridging O atoms from the (110) microfacets. These are thought to be the vacancy sites on the (110) surface, giving rise to a  $1 \times 2$  reconstruction under certain conditions.<sup>12</sup> The fourth structural model, shown in Fig. 3(b), is the simple missing-row structure suggested on the basis of the LEED symmetry and photoemission data.<sup>4</sup> Within the four models no account was taken of relaxation from the bulk atom positions.

The calculations employed PHOTON, a code based on a time-reversed dynamical LEED formalism which takes into account the two-dimensional periodicity of the surface.<sup>13</sup> It is a generalization of the PEOVER1 code<sup>14</sup> for complex surface structures. We employed input potentials obtained from a linear-muffin-tin-orbital self-consistent calculation. These potentials, which have previously been used in a band-structure calculation,<sup>15</sup> were

incorporated into a muffin-tin scheme before being used as input to the PHOTON code. The input potentials for the Ti atoms adjacent to O vacancies were empirically shifted to 1.8 eV lower binding energy, the value observed experimentally. This strategy serves to separately assess the Ti 3p photocurrent from O vacancy and other Ti sites, the latter being obtained by summing the contributions from subsequent layers until the layer contribution reached zero (in some cases up to 16 layers). As well as including multiple-scattering effects, which can be important in the low electron kinetic-energy regime, the code also takes into account the influence of the angular momentum character of the initial core state. The latter has recently been found to have a significant influence on diffraction patterns.<sup>16</sup> The branching ratio to *s*- and *d*-photoelectron waves is calculated with PHOTON.<sup>13</sup> Many-body electron effects are taken into account by a Lorentzian broadening of the initial state by 0.1 eV (FWHM) and the final state by 4 eV (FWHM). Calculations, which are for a sample at 0 K, were carried out for each of the experimental polar angle geometries over an azimuthal range  $\phi = 0^\circ$  to  $180^\circ$  in  $3^\circ$  steps. These data were subsequently averaged about  $\phi = 90^\circ$  to account for the presence of two domains, which effectively introduces a (001) mirror plane.

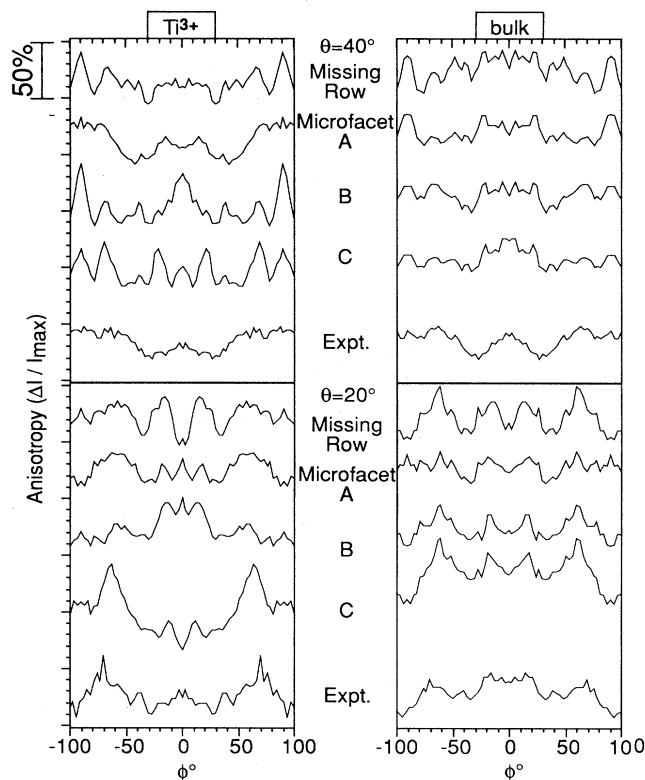


FIG. 2. Experimental PED data from  $\text{TiO}_2(100)1 \times 3$  compared with the results of multiple-scattering calculations for surface structures based on those shown in Fig. 3. Data for the bulk and  $\text{Ti}^{3+}$  features seen in Fig. 1 were obtained by curve-fitting individual spectra. Their variation with azimuthal emission angle,  $\phi$  ( $0^\circ \equiv [010]$ ), was recorded at two polar angles of emission,  $20^\circ$  and  $40^\circ$ , with respect to the surface normal. The error bar on the experimental data is estimated to be  $\pm 5\%$ .

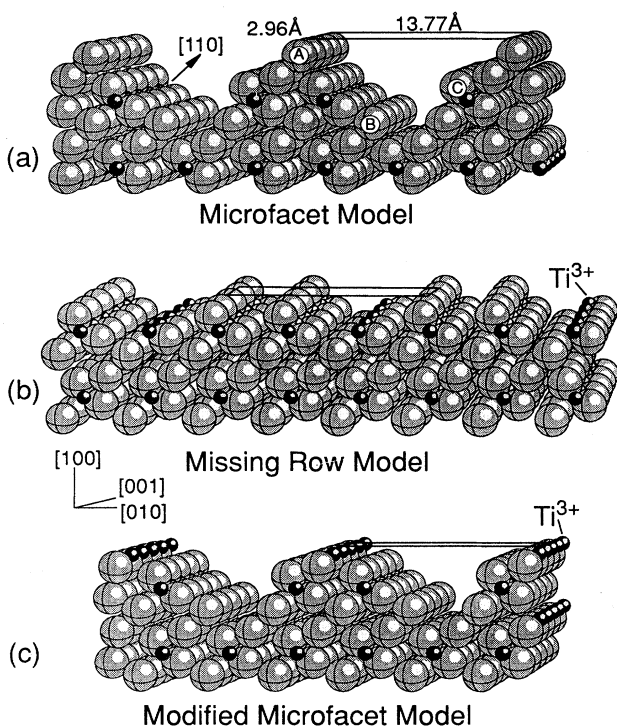


FIG. 3. Proposed models of the  $\text{TiO}_2(100)1 \times 3$  reconstruction. Small (large) spheres represent Ti (O) atoms, scaled to the appropriate ionic radii (Ref. 17). The  $1 \times 3$  unit cell is indicated. (a) Microfacet model based on the results of GXR (Ref. 5). The O atoms labeled A–C are the O-vacancy sites considered. (b) Missing-row model from LEED-photoemission measurements (Ref. 4). (c) Structure of  $\text{TiO}_2(100)1 \times 3$  derived from the data in Fig. 2.

A visual comparison of the  $\text{Ti}^{3+}$  results in Fig. 2 and the  $R$ -factor analysis<sup>11</sup> shown in Table I indicates that there is best agreement between experiment and calculations for the microfacet model with site A O vacancies. Discrepancies between experiment and the site A microfacet model calculations for the  $\text{Ti}^{3+}$  peak will probably have as a major contribution the neglect of relaxation.

TABLE I.  $R$  factors (Ref. 11) for the comparison between bulk and  $\text{Ti}^{3+}$  peak photoelectron diffraction data with the results of multiple-scattering calculations for the surface models considered. The best agreement with experiment is indicated by ●.

Model	Geometry	Bulk $\theta=20^\circ$	Bulk $\theta=40^\circ$	$\text{Ti}^{3+}$ $\theta=20^\circ$	$\text{Ti}^{3+}$ $\theta=40^\circ$
Missing row		4.34	5.87	3.33	6.58
Microfacet A		2.57	3.83	1.76●	3.10●
Microfacet B		2.52●	2.34	1.96	12.52
Microfacet C		2.95	2.05●	2.25	9.14

Although the calculations for the SCLS  $\text{Ti}^{3+}$  peak exhibit a strong model dependence, this is not the case for the bulk peak, illustrating one advantage of using the surface feature to distinguish between the possible structures. Another disadvantage of using the bulk feature is that diffraction will be significantly influenced by disorder of the type evidenced in STM images of the  $1 \times 3$  surface.<sup>3</sup> The latter contain steps edges parallel to [001] and appear to arise from the formation of extended microfacets. Their presence on the sample studied here is not accounted for in the multiple-scattering calculations, introducing discrepancies arising from the “incorrect” summation of contributions from the sides and apexes of the microfacet topology. Such discrepancies are suggested as a probable reason that a consistent result is not obtained from the bulk-feature  $R$  factors in Table I.

In summary, we have used surface core-level-shift photoelectron diffraction to locate the position of O vacancies on rutile  $\text{TiO}_2(100)1 \times 3$  by comparison with multiple-scattering calculations. The latter used as a basis the microfacet structural model derived from x-ray diffraction,<sup>5</sup> modified to include surface O vacancies. The results indicate that O vacancies occupy the top layer of the microfaceted surface, a conclusion consistent with the results of a recent STM study.<sup>3</sup> This work suggests photoelectron diffraction as a useful structural tool in the study of oxide surfaces, complementing x-ray diffraction.

This work was funded by the United Kingdom Science and Engineering Research Council.

\*Present address: Département de Chimie Appliquée et Génie Chimique, CNRS URP, 43, Bd. du 11 Novembre 1918, F-69622 Villeurbanne Cedex, France.

<sup>†</sup>Present address: Chemistry Department, University of Alabama in Huntsville, Huntsville, AL 35899.

<sup>1</sup>A. De Vita, M. J. Gillan, J. S. Lin, M. C. Payne, I. Stich, and L. J. Clarke, *Phys. Rev. Lett.* **68**, 3319 (1992).

<sup>2</sup>E. A. Colbourn, *Surf. Sci. Rep.* **15**, 281 (1992).

<sup>3</sup>P. W. Murray, F. M. Leibsle, H. J. Fisher, C. F. J. Flipse, C. A. Muryn, and G. Thornton, *Phys. Rev. B* **46**, 12 877 (1992).

<sup>4</sup>C. A. Muryn, P. J. Hardman, J. J. Crouch, G. N. Raikar, and G. Thornton, *Surf. Sci.* **251/252**, 747 (1991).

<sup>5</sup>P. Zschack, J. B. Cohen, and Y. W. Chung, *Surf. Sci.* **262**, 35

(1992).

<sup>6</sup>H. C. Poon, G. Grenet, S. Holmberg, Y. Jugnet, Tran Minh Duc, and R. Leckey, *Phys. Rev. B* **41**, 12 735 (1990).

<sup>7</sup>L. Patthey, E. L. Bullock, and K. Hricovini, *Surf. Sci.* **269/270**, 28 (1992).

<sup>8</sup>M. R. Howells, D. Norman, G. P. Williams, and J. B. West, *J. Phys. E* **11**, 199 (1978).

<sup>9</sup>P. J. Hardman, N. S. Prakash, C. A. Muryn, G. N. Raikar, G. Thornton, and S. C. Parker (unpublished).

<sup>10</sup>W. Göpel, G. Rucker, and R. Frierabend, *Phys. Rev. B* **28**, 3427 (1983); G. Rucker and W. Göpel, *Surf. Sci.* **181**, 530 (1987).

<sup>11</sup>The  $R$  factor used puts emphasis on peak positions and shape

- and is "R5" in M. A. Van Hove, S. Y. Tong, and M. H. Elcounin, *Surf. Sci.* **64**, 85 (1977).
- <sup>12</sup>M.-C. Wu and P. J. Møller, *Surf. Sci.* **224**, 250 (1989).
- <sup>13</sup>R. J. Blake, *Comp. Phys. Commun.* (to be published).
- <sup>14</sup>J. F. L. Hopkinson, J. B. Pendry, and D. J. Titterington, *Comput. Phys. Commun.* **19**, 69 (1980).
- <sup>15</sup>B. Poumellec, P. J. Durham, and G. Y. Guo, *J. Phys. Condens. Matter* **3**, 8195 (1991).
- <sup>16</sup>T. Greber, J. Osterwalder, D. Naumovic, A. Stuck, S. Hüfner, and L. Schlapbach, *Phys. Rev. Lett.* **69**, 1947 (1992).
- <sup>17</sup>R. D. Shannon, *Acta Crystallogr. Sec. A* **32**, 751 (1976).